JOURNAL OF Applied Polymer SCIENCE

Special Issue: Bioactive Surface Functionalization

Guest Editor: Prof. Koon Gee Neoh (National University of Singapore)

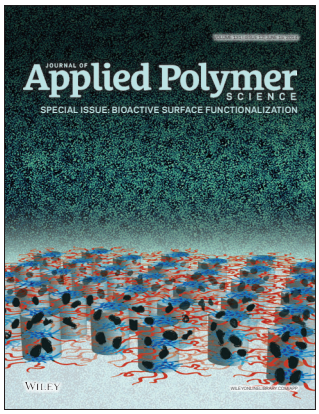

EDITORIAL

Bioactive Surface Functionalization
K. G. Neoh, *J. Appl. Polym. Sci.* 2014, **DOI: 10.1002/app.40607**

REVIEWS

Orthogonal surface functionalization through bioactive vapor-based polymer coatings
X. Deng and J. Lahann, *J. Appl. Polym. Sci.* 2014, **DOI: 10.1002/app.40315**

Surface modifying oligomers used to functionalize polymeric surfaces: Consideration of blood contact applications
M. L. Lopez-Donaire and J. P. Santerre, *J. Appl. Polym. Sci.* 2014, **DOI: 10.1002/app.40328**

Block copolymers for protein ordering
J. Malmström and J. Travas-Sejdic, *J. Appl. Polym. Sci.* 2014, **DOI: 10.1002/app.40360**

RESEARCH ARTICLES

MS-monitored conjugation of poly(ethylene glycol) monomethacrylate to RGD peptides
O. I. Bol'shakov and E. O. Akala, *J. Appl. Polym. Sci.* 2014, **DOI: 10.1002/app.40385**

Synthesis and characterization of surface-grafted poly(*N*-isopropylacrylamide) and poly(carboxylic acid)—Iron particles via atom transfer radical polymerization for biomedical applications
J. Sutrisno, A. Fuchs and C. Evrensel, *J. Appl. Polym. Sci.* 2014, **DOI: 10.1002/app.40176**

Deposition of nonfouling plasma polymers to a thermoplastic silicone elastomer for microfluidic and biomedical applications
P. Gross-Kosche, S. P. Low, R. Guo, D. A. Steele and A. Michelmore, *J. Appl. Polym. Sci.* 2014, **DOI: 10.1002/app.40500**

Regeneration effect of visible light-curing furfuryl alginate compound by release of epidermal growth factor for wound healing application
Y. Heo, H.-J. Lee, E.-H. Kim, M.-K. Kim, Y. Ito and T.-I. Son, *J. Appl. Polym. Sci.* 2014, **DOI: 10.1002/app.40113**

Bioactive agarose carbon-nanotube composites are capable of manipulating brain–implant interface
D. Y. Lewitus, K. L. Smith, J. Landers, A. V. Neimark and J. Kohn, *J. Appl. Polym. Sci.* 2014, **DOI: 10.1002/app.40297**

Preparation and characterization of 2-methacryloyloxyethyl phosphorylcholine (MPC) polymer nanofibers prepared via electrospinning for biomedical materials
T. Maeda, K. Hagiwara, S. Yoshida, T. Hasebe and A. Hotta, *J. Appl. Polym. Sci.* 2014, **DOI: 10.1002/app.40606**

Nanostructured polystyrene films engineered by plasma processes: Surface characterization and stem cell interaction
S. Mattioli, S. Martino, F. D'Angelo, C. Emiliani, J. M. Kenny and I. Armentano, *J. Appl. Polym. Sci.* 2014, **DOI: 10.1002/app.40427**

Microtextured polystyrene surfaces for three-dimensional cell culture made by a simple solvent treatment method
M. E. DeRosa, Y. Hong, R. A. Faris and H. Rao, *J. Appl. Polym. Sci.* 2014, **DOI: 10.1002/app.40181**

Elastic biodegradable starch/ethylene-co-vinyl alcohol fibre-mesh scaffolds for tissue engineering applications
M. A. Susano, I. B. Leonor, R. L. Reis and H. S. Azevedo, *J. Appl. Polym. Sci.* 2014, **DOI: 10.1002/app.40504**

Fibroblast viability and inhibitory activity against Pseudomonas aeruginosa in lactic acid–grafted chitosan hydrogels
A. Espadín, N. Vázquez, A. Tecante, L. Tamay de Dios, M. Gimeno, C. Velasquillo and K. Shirai, *J. Appl. Polym. Sci.* 2014, **DOI: 10.1002/app.40252**

Surface activity of pepsin-solubilized collagen acylated by lauroyl chloride along with succinic anhydride
C. Li, W. Liu, L. Duan, Z. Tian and G. Li, *J. Appl. Polym. Sci.* 2014, **DOI: 10.1002/app.40174**

Collagen immobilized PET-g-PVA fiber prepared by electron beam co-irradiation
G. Dai, H. Xiao, S. Zhu and M. Shi, *J. Appl. Polym. Sci.* 2014, **DOI: 10.1002/app.40597**

Journal of Applied Polymer Science

Microtextured Polystyrene Surfaces for Three-Dimensional Cell Culture Made by a Simple Solvent Treatment Method

Michael E. DeRosa, Yulong Hong, Ronald A. Faris, Hongwei Rao
Science and Technology Division, Corning Incorporated, Corning, New York 14831-0001, United States
Correspondence to: M. E. DeRosa (E-mail: derosame@corning.com)

ABSTRACT: This article describes a solvent treatment process for transforming standard flat polystyrene surfaces into textured microenvironments for three-dimensional (3D) cell culture. The process can be used with off-the-shelf microplates having 6, 12, 96, or even 384-well formats and completed in a few steps. The surface microtexture resembles tightly packed, non-interconnected micropores having a median pore size of either 115 or 19 μm depending on the strength of the solvent mixture. Hansen solubility parameter analysis was used to map out the polymer–solvent interaction conditions necessary for creating the surface texture. Primary human hepatocytes cultured on two-dimensional control surfaces attached with a flat monolayer morphology while those cultured on surfaces having 115 μm-sized pores exhibited a round 3D morphology. The cells also showed more in-vivo like behavior on the porous surface by exhibiting significantly higher basal enzymatic activity and expressing higher levels of several drug metabolism-related genes. © 2013 Wiley Periodicals, Inc. J. Appl. Polym. Sci. **2014**, *131*, 40181.

KEYWORDS: biomaterials; polystyrene; porous materials; surfaces and interfaces; thermoplastics

Received 7 August 2013; accepted 8 November 2013
DOI: 10.1002/app.40181

INTRODUCTION

Cell culture experiments typically use thermoplastic plates having two-dimensional (2D) well bottoms. When cells adhere and grow on 2D surfaces they often spread flat and consequently critical cell functions such as metabolism, gene expression, enzyme activity, differentiation, protein secretion, etc. are different than they are in living tissue. Therefore, a great deal of effort has gone into developing new microenvironments that induce cells to take on a three-dimensional (3D) morphology, which results in more *in vivo*-like behavior and more biologically relevant assays.[1–7]

Though 3D cell culture is advancing with various materials and microstructures, standard 2D plates made of polystyrene are still most commonly used. A 3D cell culture plate made of polystyrene in a conventional, inexpensive format could be an attractive technology since cultures could then be conducted on the same material as cell biologists have been using for decades. Polystyrene 3D cell culture technologies have been reported[8–10] and some are even commercially available.[11,12] However, some of these approaches[10] could be impractical to manufacture while commercially available porous inserts[11,12] are significantly more expensive than standard 2D plates.

One potentially simple and inexpensive way of making textured polystyrene plates for 3D cell culture is to use a solvent treatment process. It is known that certain organic liquids can form microcracks and voids when they contact glassy thermoplastic polymers[13–17]* and surface textures generated in this manner could be useful for enhancing cell function. We recently used a similar method to make microporous microfluidic devices on polystyrene film[18] and the same treatment could be used on injection-molded polystyrene plates.

One cell type that could potentially exhibit enhanced function from such a textured surface is primary human hepatocytes. Primary hepatocytes have been used for the last decade as the "gold standard" *in vitro* model for investigating drug-induced liver injury of new chemical entities. However, maintaining hepatocyte function *in vitro* remains a very challenging task. It has been reported that when hepatocytes are cultured under 2D conditions, they lose some key liver functions, such as phase I/II metabolism enzymes, by approximately 50% during the first 24 to 48 h in culture.[19] However, recent studies have shown that hepatocytes cultured on various 3D microtextured surfaces

*ASTM D 7474-08 Standard practice for determining residual stresses in extruded or molded sulfone plastic (SP) parts by immersion in various chemical reagents.

Additional Supporting Information may be found in the online version of this article.

have the potential to overcome the limitations caused by a 2D environment.[8,20–25]

The objective of our study is to determine if organic solvents can be used as a simple means to create microtextured surface features for 3D cell culture. We used off-the-shelf polystyrene cell culture plates as the starting substrates and mixtures of miscible good and poor solvents for polystyrene to determine the conditions necessary for creating these features. Primary human hepatocytes were used as a model system to test whether these microfeatures could enhance cell function.

EXPERIMENTAL

Solvents Used for Surface Treatment

We used 26 solvents on molded polystyrene plates to test polymer/solvent interactions. The following solvents were used as received without further purification (Fisher Scientific or Sigma Aldrich): isoamyl acetate; 1,1-dichloroethane; 1,3-dioxolane; 1,1,1-trichloroethane; methyl ethyl ketone; ethyl acetate; diethyl ether; *N*-methyl-2-pyrrolidone; acetone; toluene; chlorobenzene; *n*-butyl acetate; tetrahydrofuran; dichloromethane; cyclohexanone; glycerol; dimethyl sulfoxide; ethyl lactate; cyclohexane; methanol; 1-butanol; 2-propanol; deionized water; ethanol; propylene carbonate. All polymer/solvent interaction tests for Hansen solubility parameter (HSP) analysis were conducted on a polystyrene six-well plate (Corning, Costar® product #3736)

Biological Materials

Cryopreserved primary human hepatocyte (Lot Hu4175), CHRM® recovery medium and Thawing/Plating medium, Quant-iT™ RiboGreen® RNA Reagent, custom designed TaqMan® Low Density Arrays (TLDA) and TaqMan® Gene Expression Cells-to-C_T™ kit were purchased from Life Technologies (Grand Island, NY). Corning® Hepatocyte Maintenance Medium was obtained from Corning Life Science Mediatech (Manassas, VA). RNeasy Mini kit was purchased from Qiagen (Valencia, CA). P450-GLO™ 3A4 assay kit was obtained from Promega (Madison, WI). Type I collagen-coated microplates were purchased from BD Biosciences (San Jose, CA). Rifampicin (RIF) was purchased from Sigma-Aldrich (St. Louis, MO).

Birefringence Measurement

A modified version of a standard optical birefringence method (ASTM D4093-95) was used to qualitatively characterize the residual orientation in the wells of the polystyrene plate from the molding process. A plate was placed between a polarizer and analyzer in a manner to find the principal strain orientation in the specimen. Once the principle strain direction was found, the plate was rotated 45° to the polarizer and analyzer to observe the birefringence pattern that revealed the maximum strain in the parts. Quantitative values of the birefringence were manually measured in the rectangular polystyrene plate by determining the fringe number and optical retardation value of each fringe. The birefringence was calculated by dividing the retardation by the plate thickness.

Procedure for Making Microporous Polystyrene Surfaces on Rectangular Polystyrene Plate

One side of an injection-molded polystyrene rectangular plate (108 mm × 72 mm × 0.7 mm) (Received from Corning Life Sciences manufacturing plant, Kennebunkport, ME) was masked with a single-sided adhesive film to prevent exposure to the solvent. The plate was submerged for 30 s into a 400 mL bath containing mixtures of tetrahydrofuran/deionized water with volume ratios of 35/65, 40/60, 43/57, and 50/50. A separate plate was used for each solvent mixture. The plate was removed from the bath and immediately blow dried with nitrogen for 1–2 min. The backside adhesive film was removed after drying.

Procedure for Making Microporous Polystyrene Six-Well Plate

Large and small pore size textures were made on non-treated polystyrene six-well plates (Corning, Costar®, product #3736). The large pore texture was made by pipetting 1.5 mL of 60/40 volume mixture of tetrahydrofuran/water into each well of the plate. After 30 s, the solvent was removed and the plate was blow dried for 1–2 min. Small pore plates were made by pipetting 1.5 mL of a 40/60 volume mixture of tetrahydrofuran/isopropanol into each well. The solvent was removed after 30 s and the plate was blow dried for 1–2 minutes. Residual THF was removed by vacuum stripping the plates overnight at 84.7 kPa vacuum at 50°C. The plates were then oxygen plasma treated for 60 s at 50 W in a plasma chamber (Model MPS-300, March Instruments Inc.).

Procedure for Making Microporous 96-Well Plate

Large pore plates [Figure 2(i)] were made using non-treated 96-well plates (Corning, Costar®, product #3915). 200 mL of a 50/50 volume mixture of tetrahydrofuran/water was added to each column using an eight-channel multipipetter (Rainin Instrument, LLC). After 30 s, the solvent was removed and the wells were blow dried with nitrogen for 1–2 min. The process was repeated for all columns. Plates were then vacuum-stripped and oxygen plasma treated as described above.

Procedure for Making Microporous 384-Well Plate

Large pore plates [Figure 2(k)] were made using non-treated 384-well plates (Corning, Costar® product #3540). 25 μL of a 50/50 THF/water mixture was pipetted into all 384 wells simultaneously using a 384 channel simultaneous pipettor instrument (CyBi®-Well, CyBio AG). After 30 s, the solvent was removed and blow dried with nitrogen for 1–2 min. Plates were then vacuum-stripped and oxygen plasma treated as described above.

Procedure for Making Porous Plates for Enzyme Activity Tests

Porous 96-well plates for CYP3A4 enzyme activity testing of hepatocytes were made in two parts. A rectangular injection-molded polystyrene plate [shown in Figure 1(b) and described above] was used as the bottom of the 96-well plate. After the rectangular bottom section was textured, it was attached to a 96-well holey plate with an adhesive gasket to make the final cell culture plate.

Adhesive cellophane tape was used to mask one side of the rectangular insert plate and the excess tape was trimmed off. The masking was done to allow pores to be formed on only one side of the plate, which improves cell visibility. The plate was then flipped over and a 96-well double-sided adhesive gasket was adhered to the face of the plate. The adhesive gasket was

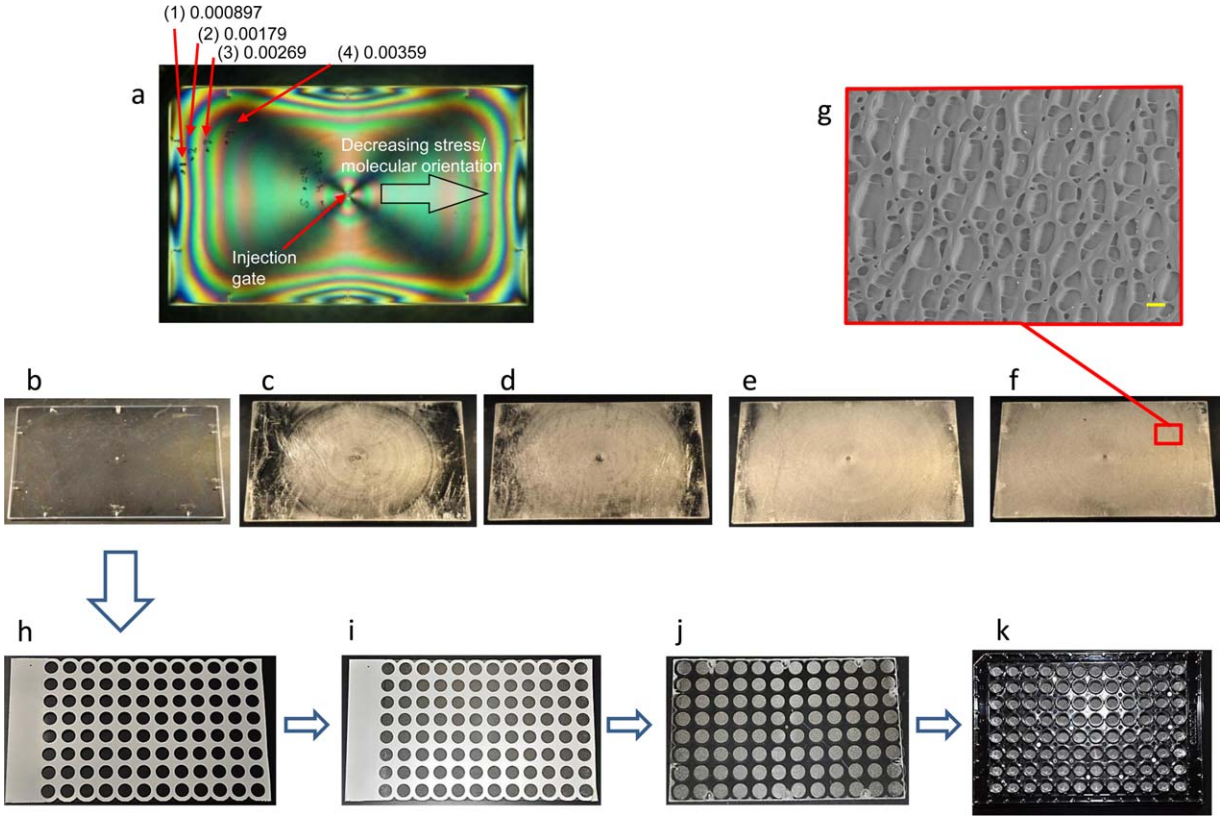

Figure 1. (a) Injection molded polystyrene plate (108 mm × 72 mm × 0.7 mm) between cross-polarizers showing fringes 1–4 and corresponding birefringence value. The mold gate is in the center of the part. (b) Plate shown in (a) with no solvent treatment. One side of the plate was treated for 30 s with a tetrahydrofuran/water mixture having the following volume ratios: (c) 35/65, (d) 40/60, (e) 43/57, and (f) 50/50. (g) SEM image showing the morphology of the surface of the 50/50 THF/water treated surface at 50× magnification. Scale bar equals 100 μm. (h) Polystyrene plate shown in image (b) with a 96-well adhesive gasket applied. (i) Plate with gasket after treatment with 50/50 THF/water mixture. (j) Adhesive gasket protective film removed to reveal textured well bottom areas. (k) Textured polystyrene plate in (j) attached to bottom of 96-well holey plate with adhesive gasket. [Color figure can be viewed in the online issue, which is available at wileyonlinelibrary.com.]

used as a stencil to allow porous patterning of the well bottoms, which were exposed to the solvent. The plate was immersed in a bath of either 60/40 THF/water or 40/60 THF/IPA to make the desired pore size. Only four of the eight rows were immersed in the solvent mixture for 30 s. The plate was removed from the bath and blow dried with nitrogen for approximately 60 s. The back adhesive masking tape was removed and the plate was vacuum-dried in an oven overnight at 50°C at 84.7 kPa vacuum to remove residual solvent.

After the bottom inserts were removed from the vacuum oven the 96-well plate was assembled. First, the plastic front side protective sheet from the adhesive gasket was removed. The plate with four rows of porous well bottoms were aligned and pressed onto a 96-well holey plate. The final plate had four rows of flat (2D) wells to serve as the 2D control and four rows of either large or small porous wells. The assembled plate was then oxygen plasma treated for 60 s at 50 W. Table I shows the nomenclatures used for surfaces used for cell culture tests.

Porous Plates for Gene Expression Testing

Microporous 12-well plates were made for conducting gene expression tests of primary human hepatoctyes. 1.2 mL of 60/40 THF/water solution was pipetted into one of the wells of a non-treated polystyrene 12-well plate (Corning, Costar®, product #3737). After 30 s, the solution was removed and the plate was blow dried with nitrogen for 1–2 min. The same procedure was used for making small pores using the 40/60 THF/IPA solution. The plates were placed in a vacuum oven at 50°C overnight at 84.7 kPa vacuum to remove residual solvent. Each plate was oxygen plasma treated for 60 s at 50 W.

Primary Human Hepatocyte Cell Culture

Cryopreserved primary human hepatocytes were thawed and purified according to the manufacturer's protocol. The purified hepatocytes were then resuspended in Corning® Hepatocyte Maintenance Medium supplemented with 10% fetal bovine serum (FBS) and plated at a density of 60,000/well in 96-well plates. The hepatocytes were allowed to attach to the surface by incubating overnight at 37°C, 95% humidity and 5% CO_2. After the heptocytes attached to the surface, 10% FBS supplemented Corning® Hepatocyte Maintenance Medium was replaced with serum free Corning® Hepatocyte Maintenance Medium. Matrigel™ overlay was performed 18–24 h after seeding. The final concentration of overlaid Matrigel™ was 0.25 mg/mL. The hepatocytes were maintained for 7 days before assay. Every 48

Table I. Nomenclature for Cell Culture Surfaces

Surface	Description
COL	2D surface with collagen I coating
MOL	2D surface with collagen I coating and Matrigel overlay
P-2D	2D surface plate with no coating
PL-3D	3D surface plate with large pores, no coating
PS-3D	3D surface plate with small pores, no coating

h, the medium was replaced with fresh Corning® Hepatocyte Maintenance Medium.

Cytochrome P450 3A4 Enzymatic Assay

The enzymatic activity of Cytochrome P450 subtype 3A4 was measured using a luminescent method. Primary human hepatocytes cultured in 96-well plates were incubated with 60 μl Corning® Hepatocyte Maintenance Medium containing 1:1000 dilution of a 3A4-specific luminogenic CYP450 substrate, Luciferin-IPA. After 1 h incubation, 50 μL of the reaction medium were mixed with 50 μL of P450-Glo™ Luciferin Detection Reagent. After incubating for 15 min, the intensity of luminescent was measured using a Victor III luminometer (Perkin-Elmer, Wellesley, MA).

Reverse-Transcription and Quantitative Real-Time PCR

Total RNA of hepatocytes cultured in each 12- or 96-well plates was isolated using RNeasy mini kit. The concentration of purified total RNA was quantified using the Quant-iT Ribogreen RNA Reagent Kit according to the manufacture protocol. A two-step RT-PCR reaction was then conducted according to TaqMan® Gene Expression Cells-to-C_T™ kit protocol. Briefly, for each sample, 16 ng of total RNA was used to transcribe to cDNA in a 50 μL RT reaction. The entire 50 μL product of the RT reaction was then mixed with 50 μL TaqMan® Gene Expression Master Mix to make PCR reaction mixture. The entire 100-μL PCR reaction mixture was then loaded into ports of a TLDA card. TLDA cards were custom-made by Applied Biosystems and contained probes in triplicates for the detection of 16 genes. PCR amplified products were detected by real-time fluorescence on an ABI PRISM 7900HT Fast Sequence Detection System (Perkin Elmer, Wellesley, MA).

Real-Time PCR Data Analysis

Quantitation of the target cDNAs, to assess basal gene expression level, were normalized to an endogenous control gene HPRT1 ($C_{T\ \text{target}} - C_{T\ \text{HPRT1}} = \Delta C_T$). The difference in expression level of each target cDNA in hepatocytes cultured on testing plate was expressed relative to that in hepatocyte cultured on collagen I plate ($\Delta C_{T\ \text{testing plate}} - \Delta C_{T\ \text{collagen I plate}} = \Delta\Delta C_T$). Fold changes in target gene expression level were determined by taking 2 to the power of this number ($2^{-\Delta\Delta C_T}$).

RESULTS AND DISCUSSION

Surface Texturing of Injection Molded Polystyrene Plates

Figure 1 shows how solvent strength and residual stress both are required to form a surface microtexture on a molded rectangular plate of polystyrene. The plate was molded with the gate in the center of the part and the birefringence pattern indicates the degree of molecular orientation and residual stress from the molding process. The fringe number along with the corresponding birefringence value is indicated in the image. The highest residual stress and molecular orientation is at the center and decreases toward the edge. The entire plate surface was exposed to a solvent mixture comprised of a "good" solvent for the polystyrene (tetrahydrofuran, THF) and a miscible "poor" solvent (water). At a low THF/water volume ratio (35/65), only the center of the plate became textured where the residual mold stress was highest. Little to no porosity was formed on the outer edges of the plate where the stress was lowest. These lower stress regions could be made porous by strengthening the mixture by adding more THF until the entire plate became porous even at the edges using a ratio of 50/50 THF/water.

Figure 1 also shows how textured multiwell plates could be made using a stenciling process. A rectangular plate was first masked on one side with tape to prevent solvent exposure. Then, a 96-well adhesive gasket was applied to the opposite side. The plate was then immersed in a 50/50 THF/water mixture for 30 s, blow dried with nitrogen, and vacuum-stripped overnight. The back masking film and adhesive gasket protective film were removed and the plate was adhered to a 96-well holey plate to form the fully assembled part.

Instead of using a stenciling process, porous microplates could be made in a much simpler fashion using off-the-shelf 2D microplates. Figure 2 shows a 6, 96, and even a 384-well microplate that were textured using a solvent mixture. In each case, the solvent mixture was added to individual wells or into all wells simultaneously to texture the entire plate. After the solvent was removed and the plate was dried, it was oxygen plasma treated to make the surface hydrophilic for improved cell attachment. The plates could also be sterilized with a conventional gamma irradiation process without degrading the texture.

We observed that two types of porous texture could be made based on the poor solvent used. For example, when THF was blended with isopropanol (40/60 THF/IPA) we produced a "small" pore texture and the polystyrene became opaque with a white color. Figure 2(c,e,f) shows an example of one well of a six-well plate that was treated in this manner to produce the small pore texture. The median pore diameter of this type of surface was found to be 19 μm by mercury intrusion volume measurement. When water was used as the poor solvent, we obtained a "large" pore texture and the polystyrene remained transparent. Figure 2(d,g,h) shows an example of one well of a six-well plate that was treated with a 60/40 THF/water mixture to make the large pore texture. Large pores made with this solvent mixture had a median pore diameter of 115 μm by mercury intrusion volume measurement. The height of the texture was measured to be 80–100 μm using optical microscopy. Solvent wicking tests revealed that both the large and small pore textures were not interconnected, but densely packed microcraters. Currently, we do not understand how the poor solvent controls the pore size or the opacity of the polystyrene. Water was the only poor solvent that produced transparent porous textures with large features. All other poor solvents produced small pores and turned the polystyrene opaque.

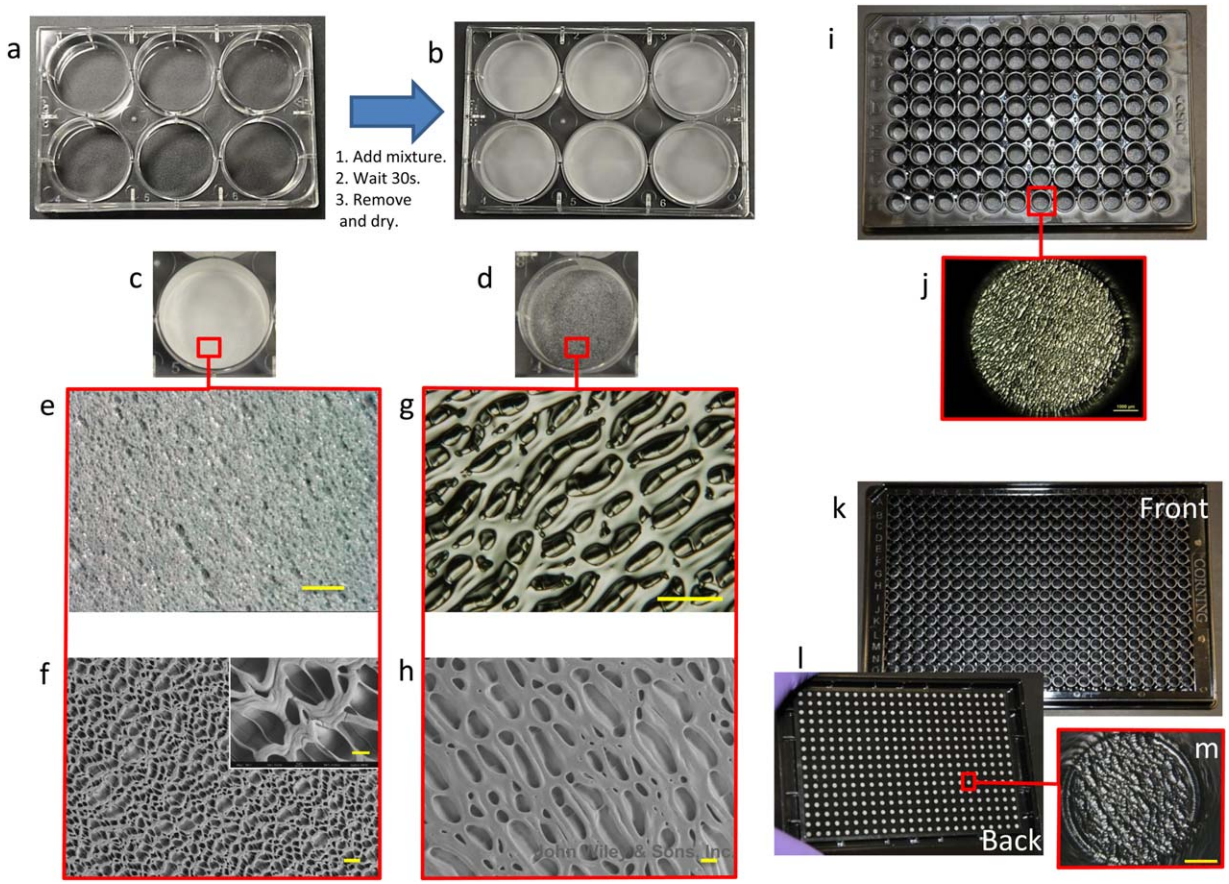

Figure 2. (a) Polystyrene six-well plate (Corning, Costar®, 3736) before solvent treatment and (b) after all six well bottoms were treated for 30 s with a 40/60 tetrahydrofuran/isopropanol mixture. (c) Optical image of one well of the six-well plate that was treated with 40/60 tetrahydrofuran/isopropanol. (d) Optical image of one well of a six-well plate that was treated with a 60/40 tetrahydrofuran/water mixture for 30 s. (e) Stereomicroscope image of the well bottom shown in (c). Scale bar is 265 μm. (f) 50× magnification SEM image of the well bottom texture shown in (e). Scale bar is 100 μm. Inset image shows the same texture in (f) but at 500×. Scale bar is 25 μm. (g) 50× magnification stereo backlit optical image of textured well bottom shown in (d). Scale bar is 500 μm. (h) 50× magnification SEM image of the well bottom texture shown in (g). Scale bar is 100 μm. (i) 96-well plate treated (Corning, Costar® 3915) with 50/50 tetrahydrofuran/water and (j) optical image of porous well bottom shown in (i). Scale bar is 1000 μm. (k) 384-well plate (Corning, Costar® 3542) after all wells were treated with a 50/50 tetrahydrofuran/water mixture for 30 s. (l) Back view of plate in (k). (m) Optical image of porous well bottom shown in (l). Scale bar is 500 μm. [Color figure can be viewed in the online issue, which is available at wileyonlinelibrary.com.]

Solvent Conditions for Making Textured Surfaces

Figure 1 illustrates how porous surface textures can be formed by tuning the solvent strength of the liquid that comes in contact with molded polystyrene as long as there is sufficient residual mold stress. An earlier study by Sung et al.[26] also showed that microporous surfaces could be made by solvent treating molded polymers. These investigators made open cell microporous features on polymethylmethacrylate with various solvents and mixtures of solvents. They found that molecular orientation formed during extrusion was required to form the pores. In their study, they chose to use a single Hildebrand solubility parameter to characterize the conditions for pore formation, but this approach was only partially successful. Here, we instead use 3D Hansen solubility parameters (HSP) to better characterize the solvent properties required for making textured surfaces.

HSP are given for three primary intermolecular forces: atomic dispersion forces (δ_D), molecular permanent dipole–dipole interactions (δ_P), and molecular hydrogen bonding interactions (δ_H).[27] The strength of polymer–solvent interactions are determined by comparing the Hansen parameters of the polymer to that of the solvent by the term R_a

$$R_a^2 = 4(\delta_{D_2} - \delta_{D_1})^2 + (\delta_{P_2} - \delta_{P_1})^2 + (\delta_{H_2} - \delta_{H_1})^2 \quad (1)$$

where subscripts 1 and 2 refer to the solvent and polymer, respectively. A good solvent has parameters that are closely matched to the polymer and results in a relatively small value of R_a. R_a increases as the solvent becomes more dissimilar to that of the polymer. Eventually, the solvent becomes poor above a threshold value of R_a defined as R_o. The relative energy difference (RED) between the polymer and solvent is defined as R_a/R_o. When the RED < 1, the solvent will dissolve the polymer and when the RED > 1 the solvent has no effect. Solvents that have a RED value near 1 only cause swelling and typically induce environmental stress cracking and crazing (ESC).

ESC of thermoplastics has been studied for many years.[13–17*] ESC occurs when a glassy polymer is placed under a tensile

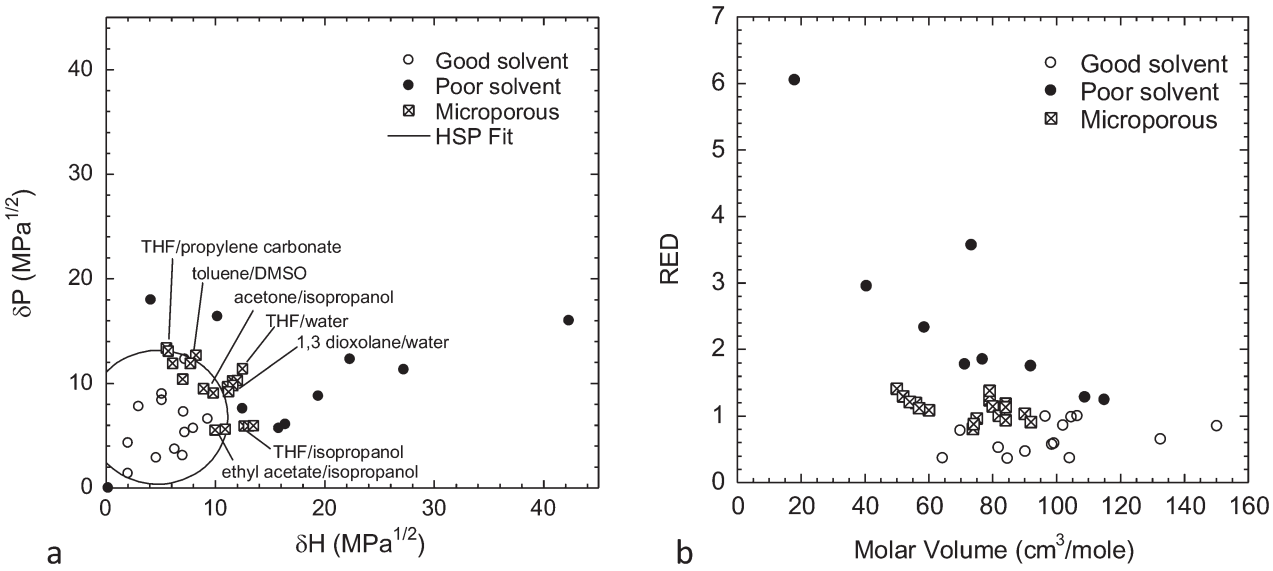

Figure 3. (a) Hansen parameter plot of δP versus δH for solvents and solvent mixtures tested on the well bottom surface of a polystyrene six-well plate. The black circular line is a cross-section of the solubility sphere fit between good and poor solvent. The following solvent mixtures with the corresponding volume ratio ranges formed microporous textures: tetrahydrofuran/water 50/50–65/35, tetrahydrofuran/isopropanol 35/65–45/55, tetrahydrofuran/propylene carbonate 37/63–50/50, ethylene acetate/isopropanol 60/40–70/30, toluene/dimethyl sulfoxide 25/75–30/70, acetone/isopropanol 70/30–80/20. (b) Relative energy difference (RED) values of all solvents and mixtures shown in Figure 3(a), versus their molar volume.

load and put into contact with a liquid. The load can be externally applied or the result of residual stress locked in during the cooling phase of a process such as injection molding. If the liquid has the right properties it will plasticize the polymer and cause yielding which accelerates local void formation. The magnitude of ESC depends on the amount of stress in the material coupled with the solvent strength of the liquid. ESC is usually undesirable and most applications try to prevent it.

We determined the interaction strength between a molded polystyrene six-well plate and various solvents and solvent mixtures in the following manner. We examined the surface of a well bottom after applying a drop of a particular solvent or mixture to see if it dissolved the surface to form a viscous liquid (good solvent), formed pores (microporous), or had no effect (poor solvent). The HSP of all the test solvents were obtained from tabulated values.[27,28] In the case of water, there are several sets of HSP values that have been reported. As an individual component, we used values for water as a single molecule and for solvent mixtures using water we used values indicated for total miscibility.[27] Solubility parameters for mixtures were calculated as a weighted volume average. δ_D, δ_P, and δ_H values of the solvents were plotted as x, y, and z coordinates, respectively, and a sphere was fit at the boundary between good and poor solvents using commercially available software.[28] The fit yielded the center of a sphere with the radius R_o. HSP values of the polystyrene plate were determined to be $\delta_D = 16.98$ MPa$^{1/2}$, $\delta_P = 6.76$ MPa$^{1/2}$, $\delta_H = 4.73$ MPa$^{1/2}$ with $R_o = 6.4$. HSP values of all solvents and solvent mixtures are given in Supporting Information Table S1.

Figure 3(a) shows a 2D plot of δ_P versus δ_H for all solvents and mixtures tested on the six-well plate surface. The circular fit is a cross-section of the sphere with $R_o = 6.4$. As the plot shows, six miscible solvent mixtures formed microporous textures and all of these mixtures were on the solubility boundary of good and poor solvent strength. The RED value which takes all three Hansen parameters into account is shown versus molecular volume in Figure 3(b) and Supporting Information Table S1. All the mixtures that formed porous textures have RED values in the range 0.9–1.4, which is similar to liquids reported to cause environmental stress crazing.[29]

Though porous textures were formed with solvent mixtures having a RED value near 1, there are some individual solvents with a RED value near 1 that did not make porous textures. In Figure 3(b) samples labeled as good solvents near a RED value of 1 include *N*-methyl pyrrolidone, diethyl ether, toluene, chlorobenzene, isoamyl acetate, and those labeled as poor solvents are cyclohexane and ethyl lactate. In the context of solvent crazing, there are other factors such as temperature, stress level, exposure time, and molecular size and shape that determine when crazing is most likely to occur.[27] It is possible that these same factors also affect the process for making porous surface textures. With regard to molecular size, cylcohexane and ethyl lactate may be too large to penetrate the surface to initiate swelling and form a porous texture under the given conditions of the experiment. Molecular size might also be a factor in the case of the solvents that were considered good but did not form porous textures. These solvents may be strong enough to slowly dissolve the topmost layer of the surface but due to their molecular size do not penetrate to a sufficient depth into the material quick enough to cause the formation of the open porous texture. Diffusion rate has been reported to be a factor in crazing,[30] but we did not examine the effect that this had on the kinetics of the pore forming process.

Our results indicate that the condition of the polymer–solvent interaction required for making the porous surface texture is

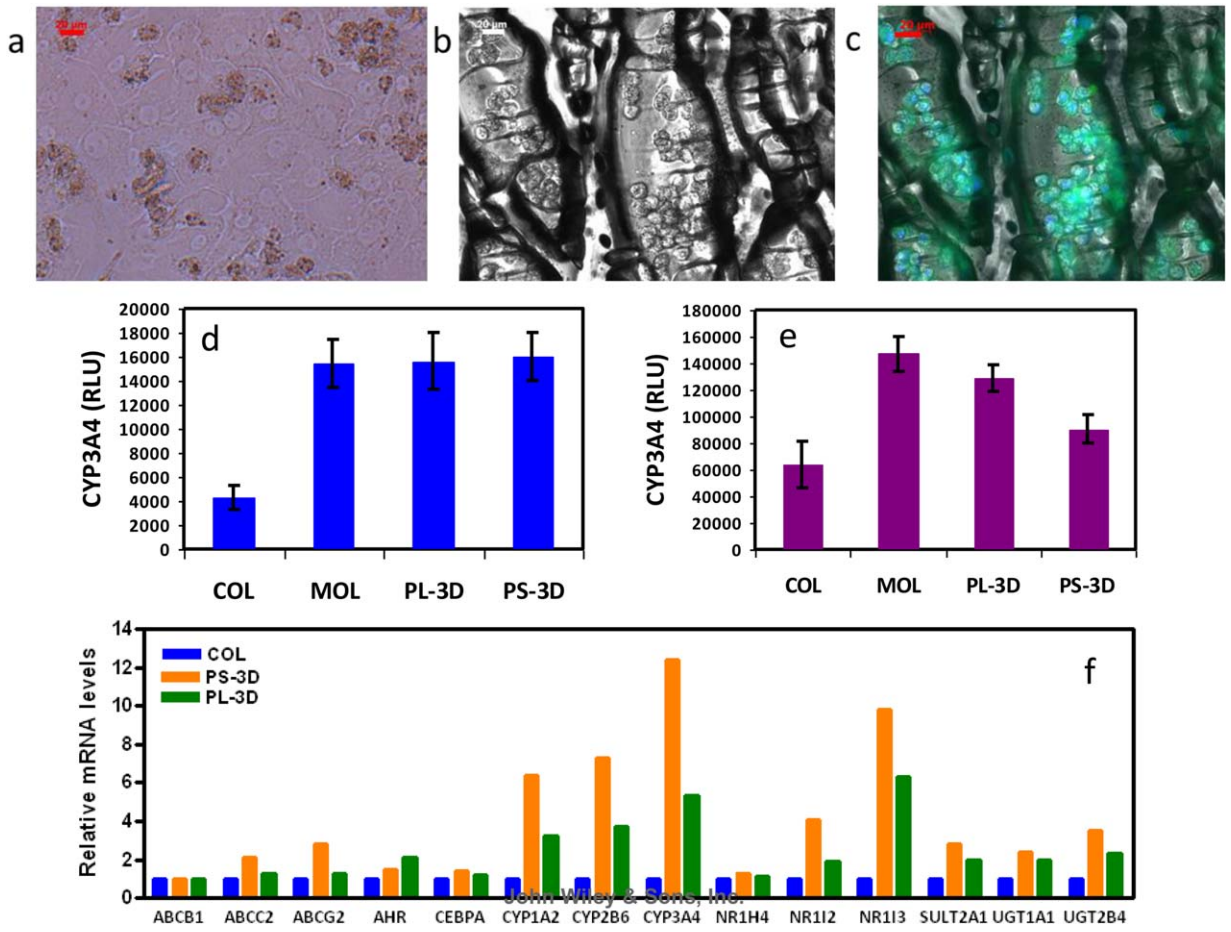

Figure 4. Standard bright field optical images of primary human hepatocytes cultured on (a) 2D polystyrene surface with a collagen I coating and (b) large pore microporous polystyrene surface with no coating. (c) Composite bright field and fluorescent image of cells stained with nuclei (blue), plasma membrane (green) on large microporous surface. [Scale bar is 20 μm in (a–c).] Non-normalized CYP3A4 (d) basal and (e) Rifampicin induced enzymatic activity of primary human hepatocytes cultured 2D collagen-coated (COL), 2D collagen with Matrigel overlay (MOL), uncoated large pore (PL-3D), and uncoated small pore (PS-3D) surface. (f) Comparison of relative gene expression profiles of primary human hepatocytes cultured on a two-dimensional collagen I-coated substrate (COL) compared to uncoated 3D surfaces with large (PL-3D) and small pores (PS-3D). [Color figure can be viewed in the online issue, which is available at wileyonlinelibrary.com.]

similar to that reported for inducing environmental stress crazing. However, the textures we made appear to be distinctly different than conventional crazes. By definition, a craze is a crack with polymer fibrils spanning the two sides of the crack which has sharp boundaries. The dimensions of cracks are usually on the order of 1 to a few tens of microns where the fibrils are typically much <1 μm in diameter.[31] The textures we formed are much larger with smoother features resembling porous foams rather than fractures. In the study by Sung et al., the authors also found that the porous surface features they formed were under similar conditions reported to cause crazing, but indicated that the pore morphology was different than crazes. They instead termed the phenomenon whitening. Since there are differences between porous surfaces and crazes, describing the pore-making process with a more general term of surface texturing other than crazing appears to be more appropriate until a deeper understanding of the mechanism of pore formation can be determined. In the next section, we describe how these porous textures were used for a cell culture application.

Cell Morphology and CYP3A4 Enzyme Activity

Hepatocytes displayed different morphologies on porous and flat surfaces. Images are only shown for large pores since the small pore texture was opaque. Cells spread flat on the 2D surface with a collagen I coating and displayed monolayer morphology with a clear cell boundary and nuclei [Figure 4(a)]. Cells adopted a spherical shape on the large microporous surface, without any coating, and were either scattered individually or formed in aggregates. The cells are approximately 20 μm in diameter and easily fit well within the crater-like features of the large pore surface texture [Figure 4(b)]. The 3D morphology of hepatocytes on the large microporous surfaces was further confirmed by fluorescence images shown in Figure 4(c).

We determined the functionality of the hepatocytes by measuring the activity level of the CYP3A4 enzyme because it is associated with 50–60% of drug biotransformation in humans.[11] Figure 4(d) shows the basal enzyme activity of hepatocytes cultured on 2D and 3D surfaces. The activity was significantly

higher on both large and small pore surface without any coating compared to a 2D surface with a collagen I coating. The activity on the large pore surface was comparable to a 2D surface with a collagen I coating and Matrigel™ overlay. Figure 4(e) shows the rifampicin induced CYP3A4 activity to evaluate how hepatocytes responded to chemical treatment on different surfaces. Cells had the highest induced activity on the 2D Matrigel overlay surface while cells cultured on both porous surfaces had significantly higher readings than the collagen I-coated 2D surface.

Overall, the enhanced function on the porous surfaces is qualitatively consistent with what has been reported for hepatocytes cultured on non-interconnected microtextured surfaces. Nakamura et al.[8] reported that a square-shaped microspace texture was able to produce 3D cell aggregation of HepG2 and primary human hepatocytes. The resulting gene expression on these surfaces was higher than cells cultured on a 2D surface coated with collagen. Sakai et al.[24] showed that well-controlled spheroids of HepG2 cells could be formed on PEG-coated cylindrical microwells and these spheroids exhibited higher protein secretion than cell monolayers grown on a 2D surface. Finally, Mori et al.[21] demonstrated that spheroids and cylindroids of rat hepatocyte and HepG2 cells could be formed on microtextured surfaces. Both the spheroid and organoid structure showed higher protein secretion and ammonia removal than the monolayer grown on a 2D collagen-coated surface.

Gene Expression Results and Analysis

In addition to measuring CYP3A4 activity, we used gene expression as another metric to evaluate a broader range of hepatocyte functions. Fourteen drug metabolism-related genes and two housekeeping genes were chosen for this study. We determined the relative gene expression levels of RNA isolated from hepatocytes by using a quantitative real-time PCR method. The 2D collagen-coated surface was compared to uncoated large pore and small pore surfaces. Figure 4(f) shows that cells cultured on both small and large pore surfaces had higher mRNA levels of several important drug metabolism enzymes than on a 2D surface with a collagen I coating. These enzymes included phase I/II metabolism enzymes (CYP1A2, CYP2B6, CYP3A4, SULT2A1, UGT1A1, and UGT2B4), transcription factors (AHR, NR1I2, and NR1I3) and drug transporters (ABCC2 and ABCG2). The gene expression results were consistent with CYP3A4 enzymatic functional assay results and our overall results are consistent with other studies that showed how microwell features improve hepatocyte function mainly by enabling cells to form 3D aggregates.[21–24]

CONCLUSIONS

In this article, we demonstrated that microtextured polystyrene surfaces for 3D cell culture can easily be made with off-the-shelf microplates by a simple solvent treatment process. The porous surface textures were formed with a combination of residual surface stress and solvent strength of the liquid contacting the surface. The conditions required to form the textures were similar to those reported to induce solvent crazing and confirmed by HSP analysis. However, the porous features formed on the surface were significantly larger than craze structures. Though not understood at this time, we observed that using water as the poor solvent in a mixture created a microporous texture with features large enough to trap and hold cells and transparent enough to observe them with standard microscopy methods. Primary human hepatocytes cultured on the porous textures exhibited higher basal enzyme activity and gene expression of numerous genes compared to cells cultured on a 2D flat surface coated with collagen. The higher function occurred on the textured surfaces even though the pores were not-interconnected. Additionally, the microporous surfaces enhanced basal cell function even without a collagen coating indicating that the physical structure of the surface had significant impact on this cell type independent of the surface chemistry. Though this study focused on hepatocytes, other cell types could be studied in the future to see the effect this texture has on their behavior.

ACKNOWLEDGMENTS

The authors thank Terri Bohart for conducting the CYP3A4 assay and data analysis and Li Liu for conducting the gene expression tests and analysis. James Price for conducting the birefringence measurement and analysis, Natalya Isachkina for the SEM images. We also would like to thank Rachelle Landolf and Deborah Smith for conducting the mercury intrusion porosity measurements and John Wang for technical discussion of the results.

REFERENCES

1. Pampaloni, F.; Stelzer, E. H. K.; Masotti, A. *Rec. Patent Biotech.* **2009**, *3*, 103.
2. Lee, J.; Cuddihy, M.J.; Kotov, N.A. *Tissue Eng. Part B.* **2008**, *14*, 61.
3. Li, Y.; Yang, S.-T. *Biotechnol. Bioprocess Eng.* **2001**, *6*, 311.
4. Flemming, R. G.; Murphy, C. J.; Abrams, G. A.; Goodman, S. L.; Nealey, P. F. *Biomaterials* **1999**, *20*, 573.
5. Weigel, T.; Schinkel, G.; Lendlein, A. *Exp Rev. Med. Devices.* **2006**, *3*, 835.
6. Shea, L. D.; Wang, D.; Franceschi, R. T.; Mooney, D. *J. Tissue Eng.* **2000**, *6*, 605.
7. Zhang, H.; Lin, C.-Y.; Hollister, S. J. *Biomaterials.* **2009**, *30*, 4063.
8. Nakamura, K.; Mizutani, R.; Sanbe, A.; Enosawa, S.; Kasahara, M.; Nakagawa, A.; Ejiri,Y.; Murayama, N.; Miyamoto, Y.; Torii, T.; Kusakawa, S.; Yamauchi, J.; Fukuda, M.; Yamazaki, H.; Tanoue, A. *J. Biosci. Bioeng.* **2011**, *111*, 78.
9. Altmann, B.; Ahrens, R.; Welle, A.; Dinglreiter, H.; Schneider, M.; Schober, A. *Biomed. Microdev.* **2012**, *14*, 291.
10. Cheng, K.; Lai, Y.; Kissaalilta, W. S. *Biomaterials.* **2008**, *29*, 2802.
11. Knight, E.; Murray, B.; Carnachan, R.; Przyborski, S. *Methods Mol. Biol.* **2011**, *695*, 323.
12. Caicedo-Carvajal, C. E.; Liu, Q.; Remache, Y.; Andre Goy, A. K.; Suh, S. J. *Tissue. Eng.* **2011**, Article ID 362326.
13. Volynskii, A. L.; Bakeev, N. F. Solvent Crazing of Polymers; Elsevier: Amsterdam, **1995**.

14. Wright, D. C. Environmental Stress Cracking of Plastics; Rapra Technology Ltd.: Shawbury, **1996**.
15. Bernier, G. A.; Kambour, R. P. *Macromolecules.***1968**, *1*, 393.
16. Kambour, R. P.; Gruner, C. L.; Romagosa, E. E. *J. Polym. Sci. Phys. Ed.* **1973**, *11*, 1879.
17. Kambour, R. P.; Gruner, C. L.; Romagosa, E. E. *Macromolecules.***1974**; *7*, 248.
18. Yuen, P. K.; DeRosa, M. E. *Lab. Chip.* **2011**, *11*, 3249.
19. Maslansky, C. J.; Williams, G. M. *In Vitro.* **1982**, *18*, 663.
20. Colette, S.; Ranucci, M. S.; Moghe, P. V. *Tiss. Eng.* **1999**, *5*, 407.
21. Wong, S. F.; No, D. Y.; Choi, Y. Y.; Kim, D. S.; Chung, B. G.; Lee, S.-H. *Biomaterials.* **2011**, *32*, 8087.
22. Mori, Y.; Sakai, Y.; Nakazawa, K. J. *Biosci. Bioeng.* **2008**, *106*, 237.
23. Nishimura, M. *Drug Metab. Pharmacokinet.* **2010**; *25*, 236.
24. Sakai, Y.; Nakazawa, K. *Acta Biomater.* **2007**, *3*, 1033.
25. Mori, Y.; Sakai, Y.; Nakazawa, K. *J. Biosci. Bioeng.* **2008**, *106*, 237.
26. Sung, N. H.; Gahan, R. E.; Haven, R. E. *Polym. Eng. Sci.* **1983**, *23*, 328.
27. Hansen, C. M. Hansen Solubility Parameters a User's Handbook, 2nd ed; CRC Press: Boca Raton, **2007**.
28. HSPiP. Hansen Solubility Parameters in Practice. Software version 3.1.12., **2008–2010**.
29. Hansen, C. M.; Just, L. *Ind. Eng. Chem. Res.* **2001**, *40*, 21.
30. Hansen, C. M. *Polym. Degrad. Stab.* **2002**, *77*, 43.
31. Chau, C. C.; Li, J. C. M. *J. Mater. Sci.* **1983**; *18*, 3047.